A Power/Hardware-Efficient SiPM Readout IC Embedded in a Boost Converter for Mobile Radiation Dosimeters

Hyuntak Jeon and Se-Un Shin, *Member, IEEE*

***Abstract*—A radiation detection system provides radiation intensity to protect human life from hazardous radiation. However, the prior portable radiation detection system (mobile radiation dosimeter) structures had a problem in that various subsystems had to be designed with complex circuits. First, since the radiation detector must be driven by a relatively high voltage, a high-efficient boost converter that can receive the battery voltage and generate a high bias voltage must be implemented. Second, sophisticated sensor interface circuits that can convert the analog signal generated by the radiation detector to digital value must also be implemented. To reduce the complexity of the mobile radiation dosimeters, a power- and hardware-efficient radiation detection system IC is presented for mobile radiation dosimeters. The current value of a silicon photomultiplier (SiPM) used as a radiation detector is sensed from the control information of a boost converter in the process of regulating a voltage to bias the SiPM. Due to this embedded sensing function, no additional hardware and power consumption are required for implementing and operating separate sensor interface circuits while providing sufficient radiation sensing performance. The implemented radiation detection system IC achieves 0.217-μA_{rms} input referred noise performance over 1-kHz signal bandwidth and 10-mA maximum allowable linear input current range. In addition, the proposed dc–dc boost converter can generate a high enough voltage (∼27 V) to drive SiPM from a lithium-ion battery with an efficiency of 72%. The irradiation test with radiation check source (^{137}Cs) demonstrates that the bias voltage is well regulated in the presence of high-energy radiation particles.**

***Index Terms*—DC-DC boost converter, mobile radiation dosimeters, sensor readout IC, silicon photomultiplier (SiPM).**

I. Introduction

NUCLEAR power plants have been the basis of modern industrial development because these plants produce large amounts of highly efficient electricity. Moreover, in modern industries that consume large amounts of electricity, nuclear power generation with a stable power supply is the most essential requirement. Furthermore, thanks to its low CO_2 generation, it also has the advantage of less air pollution compared to other fossil fuel based power generation methods. However, the initial construction cost of nuclear power plants is extremely high and the treatment of radioactive waste has been an ongoing problem. Since the recent Fukushima nuclear accidents, concerns about the safety of nuclear power plants have been raised more than before. Because failure to safely control the strong nuclear energy can lead to the most threatening accidents to human beings and environments.

It was strong enough to destroy the ecosystems, and a lot of people were exposed to radiation suffering from generation to generation. The radiation exposure over a certain level may cause biologically harmful effects, such as carcinogenesis [1], [2]. Surprisingly, we are already exposed to numerous radiation sources, even in the moments we are not aware of it. As shown in Fig. 1 [3], the radiation sources from nature are not harmful, but, artificial radiation could be extremely dangerous to humans. However, if the ecosystem itself is contaminated with radiation, we will no longer be safe from a radiation disaster. As a result, not only the nuclear power plant workers managed by competent agents but also the ordinary people in daily life

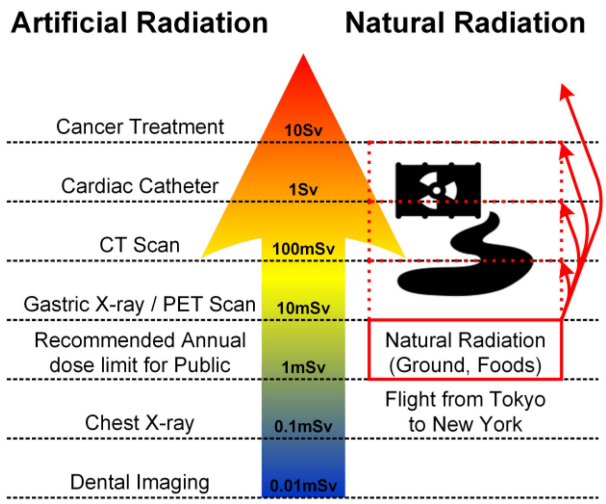

Fig. 1. Various radiation sources in modern environment.

Manuscript received 13 March 2022; revised 9 July 2022 and 27 August 2022; accepted 1 September 2022. Date of publication 9 September 2022; date of current version 10 October 2022. This work was supported by the Institute of Information & Communications Technology Planning & Evaluation (IITP) under a grant funded by the Korean government (MSIT) (2022-0-00720) for "Development of W-band compact, high-efficiency, novel RF/power components for next-generation high-speed low-orbit satellite communications." An earlier version of this paper was presented in part at the 2011 IEEE Symposium on VLSI Circuits [DOI: 10.23919/VLSICircuits52068.2021.9492346]. Recommended for publication by Associate Editor F. J. Azcondo. *(Corresponding author: Se-Un Shin.)*

Hyuntak Jeon is with the School of Electronics Engineering, Chungbuk National University, Cheongju 28644, South Korea (e-mail: ht.jeon@cbnu.ac.kr).

Se-Un Shin is with the Department of Electrical Engineering, Ulsan National Institute of Science and Technology, Ulsan 44919, South Korea (e-mail: seuns@unist.ac.kr).

Color versions of one or more figures in this article are available at https://doi.org/10.1109/TPEL.2022.3205345.

Digital Object Identifier 10.1109/TPEL.2022.3205345

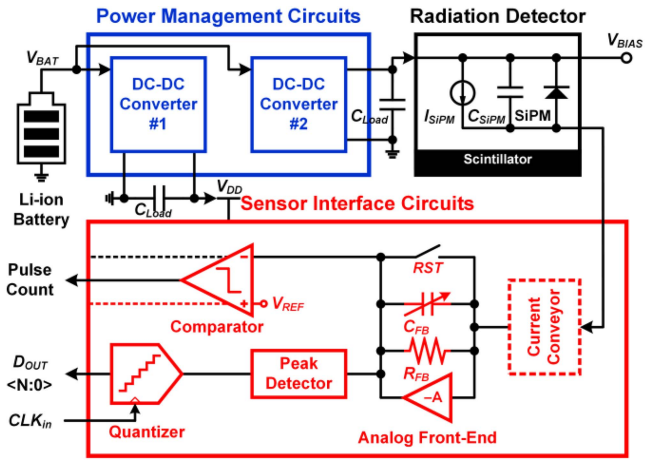

Fig. 2. Conventional radiation detection system for mobile dosimeters: separate implementation of sensor interface and power management circuits.

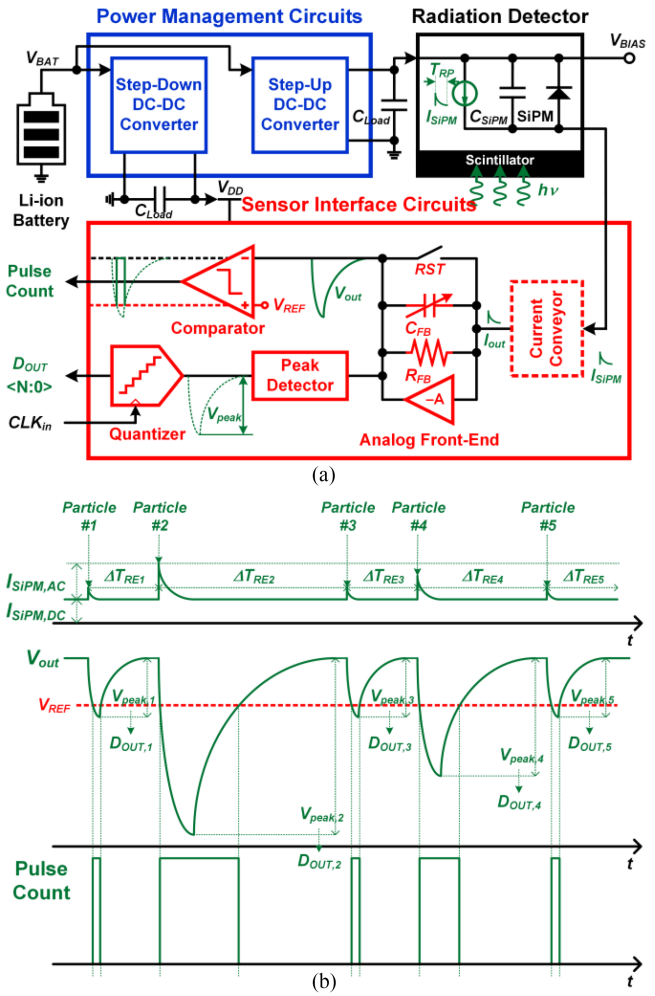

Fig. 3. Electrical analysis of mobile radiation dosimeter. (a) Basic operation. (b) Output waveforms.

are at increased risk of radiation exposure. Referring to the data measured by a radiation dosimeter, it is found that the indicators of radioactive contamination are detected at considerable levels, even in the residential environment [4]. Unfortunately, the threat of radiation is not far from our lives.

As circuit engineers, we believe that we have to protect not only the efficiency and safety of nuclear power plants but also our lives. If a radiation measurement system is developed, which can be easily used by the general public, it will help us to save our lives from radioactive contamination. Fortunately, the prior radiation detection systems could give people in daily life the opportunities to avoid being exposed to excessive radiation unconsciously [5], [6], [7], [8], [9], [10]. However, they have to be optimized to apply to mobile devices since large-volume batteries or external boards for power management must be accompanied for long-term use. In this article, we analyze the principle and operation of prior radiation detection systems. In addition, we propose a mobile radiation dosimeter that can be widely distributed to the general public by improving the problems of the conventional system.

This article is organized as follows: Section II describes and analyzes a conventional radiation detection system for mobile dosimeters, and Section III presents the key ideas and the detailed circuit implementation proposed to solve the problems of the prior mobile dosimeter structures. The measurement results of the implemented IC are discussed in Section V. Finally, Section VI concludes this article.

II. Conventional Mobile Radiation Dosimeters

Basically, the radiation measurement systems for mobile applications are constructed as shown in Fig. 2 [5], [6], [7], [8]. It consists of a silicon photomultiplier (SiPM) used as a radiation detector, sensor interface circuits, and power management circuits. First, SiPM is the most popular radiation detector, which generates radiation-induced charges. Second, the sensor interface circuits convert the charge signal into digital outputs. Third, the power management circuits provide the necessary voltages and currents to the radiation detector and sensor interface circuits. In the rest of this section, the basic operation of a general radiation detection system will be analyzed to verify the necessities of this research.

A. Radiation Detector

Thanks to its relatively low bias voltage (V_{BIAS}) and high charge generation rate, the SiPM became one of the most widely used radiation detectors in recent years [11]. We choose a commercial SiPM [12], which is suitable for mobile applications, thanks to its relatively low minimum V_{BIAS} (25.5 V) and area. Despite its compact hardware specifications, it has a sufficiently high charge generation rate to measure all radiation signals in a wide bandwidth. Furthermore, we can simply set up the radiation detector by using optical glue for physical contact between a scintillator and a bunch of photodiode cells.

After the setup for the SiPM with applying an appropriate V_{BIAS}, it is ready to operate as a radiation detector (see Fig. 3). First, the radiation particles are converted to photons through the scintillator, as plotted in Fig. 3(a). Second, the photons injected into the photodiode generate charge signals (I_{SiPM}) proportional

to the energy of the radiation particles. Finally, the charge signal of SiPM has a spike shape which soars rapidly with a short pulsewidth (T_{RP}: ~300 ns). If the injected radiation particles have strong energy, the amount of generated charges and T_{RP} will be increased. In addition, if the time intervals between the radiation events (ΔT_{RE}) are shortened, the average energy of injected radiation will be increased. In general, as the area of SiPM increases, the probability which can be injected into SiPM increases. However, it is inevitable to increase the parasitic capacitance (C_{SiPM}) and detector noise.

The specifications of the SiPM imply the most important information for optimizing the power management circuits and sensor interface circuits described later. Basically, the SiPM has to be supplied with stable and appropriate V_{BIAS} to generate reliable signal information. If V_{BIAS} is generated too high, the dc component of I_{SiPM} ($I_{\mathrm{SiPM,DC}}$) and the ac component of I_{SiPM} ($I_{\mathrm{SiPM,AC}}$) become large simultaneously, so that a large signal can be output. However, in general SiPM, it should be noted that as the signal increases, the noise called dark current also increases. Therefore, it is important to select a product that is easy to design optimized sensor interface circuits and power management circuits among various types of commercial SiPM products. Referring to [12], we selected a suitable product with maximum I_{SiPM} of 10 mA, C_{SiPM} of 1 nF, and minimum dark current of 0.3 μA performance when V_{BIAS} of 25.5 V or higher is supplied. These values will be used as the most important indicators to determine the performance of the sensor interface circuits and power management circuits for the selected SiPM.

B. Sensor Interface Circuits

In a part of Fig. 3(a), the basic operation of the conventional sensor interface circuits for SiPM is described. Basically, the sensor interface circuits generate digital outputs proportional to the value of I_{SiPM}. However, it is inefficient to process the charges using a general voltage sensing analog front-end because the radiation signal has characteristics that are much faster than the general sensor signal. Therefore, the charge-sensitive amplifier (AMP) is widely used as an analog front-end for processing radiation-induced charges in SiPM [5], [6], [7], [8]. The analog front-end in Fig. 3(a) consists of an OP-AMP, a capacitor, a resistor, and a switch. When I_{SiPM} flow to the input of the charge-sensitive AMP, the OP-AMP integrates the injected charges on the outputs as much as the closed loop gain. As a result, the amplitude of V_{out} is proportional to the injected charges as

$$\frac{V_{\mathrm{out}}}{I_{\mathrm{out}}} = \left(R_{\mathrm{FB}} || \frac{1}{sC_{\mathrm{FB}}}\right) \cdot \frac{T(s)}{1+T(s)} = \text{Gain} \cdot \text{Gain Error}. \quad (1)$$

The processed V_{out} through the charge-sensitive AMP is transferred to the peak detector and comparator. V_{peak} generated from the peak detector is converted to D_{OUT} by a quantizer. At the same time, the comparator counts the number of events. The D_{OUT} and counted pulses represent the amount of charge and the number of events, respectively. Combining D_{OUT} and the pulse counts makes it possible to finally extract the intensity information of the radiation injected to SiPM. Through the output waveforms in Fig. 3(b), the basic operations of the sensor interface circuits for continuous radiation particle signals can be confirmed. D_{OUT} and the pulse count generated by sensor interface circuits provide information on $I_{\mathrm{SiPM,AC}}$ and ΔT_{RE}, respectively.

The conventional radiation sensor interface circuits described above have serious disadvantages. First, to obtain an accurate V_{peak} value, the peak detector has to be designed with an excessively large capacitor. Because the value of V_{peak} charged in a relatively small capacitor can be decreased due to leakage current. This means that a lot of power can be wasted in the process of charging and discharging a large value capacitor for each radiation event. Second, if it is impossible to use a peak detector that consumes so much power, it may be necessary to design a high-resolution quantizer operating at an extremely high clock frequency ($\mathrm{CLK_{in}}$). However, the high-speed quantizer also consumes excessively much power, and the accuracy of the V_{peak} value is inevitably degraded. Third, since V_{peak} and counted pulse values are separately extracted, additional signal processing is required for users who need simple information about the radiation intensity. Due to these problems, the conventional radiation sensor interface circuits have made it difficult to use the mobile radiation dosimeter for a long time even though it is absolutely necessary.

C. Power Management Circuits

Power management circuits are the most important subsystems in mobile applications. Because battery-based portable devices require efficient power management circuits for long-term use. As shown in Fig. 3(a), at least two dc–dc converters are required for the basic operation of the conventional radiation detection system.

First, V_{BIAS} must be stably regulated within a maximum 10-mA load range for the basic operation of SiPM [12], as discussed above. In the mobile application, V_{BIAS} has to be regulated by using a step-up dc–dc converter that receives V_{BAT} as input. Considering the nominal bias voltage of [12], the biggest challenge in designing this converter is to be able to achieve a high conversion ratio ($V_{\mathrm{BIAS}}/V_{\mathrm{BAT}}$) of almost eight times. Second, a nominal voltage (V_{DD}) must be stably regulated for the basic operation of sensor interface circuits. Unlike V_{BIAS}, V_{DD} can be regulated by a step-down dc–dc converter with V_{BAT} as input. Considering the power consumption and signal characteristics of conventional sensor interface circuits for SiPM [5], [6], [7], [8], the most important thing to consider in designing the step-down converter is to be able to minimize the voltage ripple caused by the switching of mixed-signal circuits.

The biggest problem with power management circuits for conventional mobile dosimeters is that they need to be optimized for the radiation detector and the sensor interface circuits. Referring to the conventional mobile dosimeters [5], [6], [7], [8], the external power boards were simply used instead of a separately optimized regulator. In particular, from the performance of commercial step-up dc–dc converters [13], [14], [15], [16], [17] for V_{BIAS}, it is estimated that they were operated under unoptimized conditions. As a result, the operating time of the

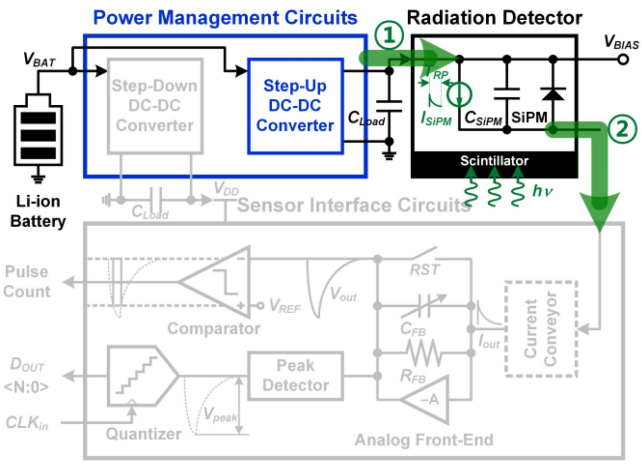

Fig. 4. Basic concept of proposed radiation detection system for mobile dosimeters.

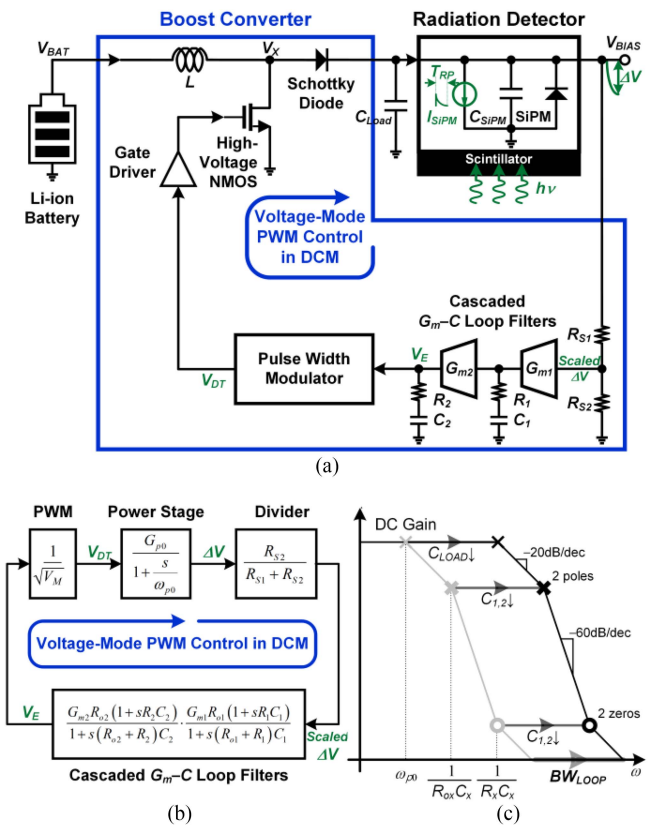

Fig. 5. Basic configuration and small-signal analysis of proposed mobile dosimeters. (a) Schematic diagram. (b) Small-signal loop analysis. (c) Frequency loop response of voltage-mode dc–dc boost converter for SiPM.

system is shortened, and the portability of the mobile dosimeter is reduced.

According to the previous analysis, a systematic solution for the conventional radiation detection system is needed to propose an optimized mobile radiation dosimeter to extend battery life. Therefore, an efficient radiation measurement system will be proposed to apply to mobile applications in the next section.

III. Proposed Mobile Radiation Dosimeters

The key concept of the mobile radiation dosimeter proposed in this research begins with the operation of the conventional system as shown in Fig. 4. If the radiation particles are injected into the SiPM, I_{SiPM}s are generated, which can be interpreted differently in terms of power management circuits and sensor interface circuits, respectively. It is natural that I_{SiPM} can be seen as currents supplied by the step-up converter of power management circuits as shown in green number ①. However, I_{SiPM} can be also seen as charges that the sensor interface circuits should detect as shown in green number ②. Ironically, these two differently interpreted currents are essentially the same information which we call the radiation-induced charges. In other words, the conventional radiation detection system consists of two different circuitries with the same information, unnecessarily. In this article, we propose to use a single circuitry for doing the same processes. If the sensing information can be obtained from the step-up dc–dc converter, there is no need to design the sensor interface circuits and even a step-down converter to drive V_{DD}. The information can be identified through how much charge it has supplied in the process of regulating V_{BIAS}.

A power- and hardware-efficient radiation detection system for mobile dosimeter is started from the basic configuration of a voltage-mode dc–dc boost converter in Fig. 5. The proposed system comprises only a radiation detector and a dc–dc boost converter, which regulates V_{BIAS} used to operate the SiPM. When a radiation particle is injected into the SiPM through the scintillator, a voltage drop (ΔV) occurs due to I_{SiPM}, and a duty signal (V_{DT}) turns ON and OFF the power switch to regulate the voltage back to the original V_{BIAS} value. Considering that the current supplied to the SiPM by the boost converter is equal to I_{SiPM} generated by the injected radiation particles, the radiation detection result can be obtained directly from the control information of the boost converter. Thanks to the proposed concept, we do not have to design the complicated sensor interface circuits and the step-down dc–dc converter to drive them.

Since the SiPM operates properly when V_{BIAS} is maintained to be higher than 25.5 V [12], the boost converter should have a sufficiently wide loop bandwidth ($\mathrm{BW_{LOOP}}$) so that V_{BIAS} can be quickly recovered before the next radiation particle is injected. Conventionally, a large external load capacitance (C_{Load}) is used to reduce the output voltage ripple, leading to a significant reduction of $\mathrm{BW_{LOOP}}$ [13], [14], [15], [16], [17]. To increase $\mathrm{BW_{LOOP}}$, a current-mode control can be employed [13], [15], [16], [17], but implementing a low-error current-sensing circuit is not straightforward and requires high power consumption, making the current-mode control approach unsuitable. Therefore, the proposed boost converter is controlled in the voltage domain, and cascaded G_m–C loop filters and a relatively small C_{Load} (16 nF) are used [see Fig. 5(a)]. The boost converter implemented in Fig. 5(a) can be composed of simple small signal models as shown in Fig. 5(b) [18]. The conventional boost converter operating in discontinuous-conduction mode (DCM) can be modeled with a one-pole power stage and a large C_{Load} acts as a dominant pole of loop gain. For the designed boost converter to always operate in DCM, the following equations

were used to calculate the boundary condition between DCM and CCM [18]:

$$\frac{2L}{R \cdot T_s} < D \cdot (1-D)^2 \tag{2}$$

$$R = \frac{V_{\mathrm{BIAS}}}{I_{\mathrm{Load}}} \tag{3}$$

$$\frac{V_{\mathrm{BIAS}}}{V_{\mathrm{BAT}}} = \frac{1}{1-D}. \tag{4}$$

Utilizing (2)–(4), the specifications ($V_{\mathrm{BAT}} = 3.7$ V, $V_{\mathrm{BIAS}} = 27$ V, $T_s = 1$ μs, $I_{\mathrm{Load}} = 10$ mA) of SiPM [12] can be calculated that the value of L has to be selected under 22.8 μH to make the boost converter set to always operate in DCM. For wide $\mathrm{BW}_{\mathrm{Loop}}$ with low gain error, the power stage operating in DCM is controlled by G_m–C loop filters [19], [20]. First, as shown in the modeling scheme in Fig. 5(a) and (b), the loop filter can be analyzed so that the series couplings of $C_{1,2}$ and $R_{1,2}$ are connected in parallel to the output of operational transconductance amplifier (OTA). When $C_{1,2}$ and $R_{1,2}$ are combined with OTA's transconductance ($G_{m1,2}$) and output impedance ($R_{o1,2}$), the transfer function of the G_m–C loop filters can be defined as shown in Fig. 5(b). By cascading a pair of G_m–C loop filters as shown in Fig. 5(a) and (b), the loop gain reduction due to sensing resistors R_{S1} and R_{S2} was compensated and the gain error could be minimized. This was to allow the feedback loop to be controlled with high accuracy unlike the conventional dc–dc boost converters. As a result, it is possible that the loop gain plot of the boost converter proposed as shown in Fig. 5(c) can be expressed as a single pole of the power stage, double poles, and zeros inserted by the cascaded G_m–C loop filters. Therefore, if C_{Load} and $C_{1,2}$ of the loop filter are reduced, $\mathrm{BW}_{\mathrm{LOOP}}$ can be extended as shown in Fig. 5(c). As a result, $\mathrm{BW}_{\mathrm{LOOP}}$ is increased up to about 100 kHz being able to be measured with high accuracy.

To obtain an accurate I_{SiPM} value from D_{OUT} over a wide range, the loop response of the boost converter should be linearized. For the conventional pulsewidth modulation (PWM) control, V_{DT} is generated by comparing the error voltage (V_E) with a sawtooth waveform (V_{ST}) [see Fig. 6(a)]. Since the output charge (Q_{OUT}) has a quadratic relationship with the duty of V_{DT}, which in turn is a linear function of V_E and hence I_{SiPM}, the overall loop response becomes quadratic. As shown in Fig. 6(a), the amount of charges supplied to the load by the boost converter operating in DCM is the same as the integral value of the I_L waveform of the freewheeling phase. Therefore, the V_{DT} generated by the conventional sawtooth waveform generator has a square relationship with Q_{OUT}. In other words, due to the nonlinear relationship between V_E and Q_{OUT}, it can be concluded that the information about Q_{OUT} obtained through the nonlinear loop response is unreliable. For example, if V_E is doubled, V_{DT} will be doubled, but V_E will be quadrupled. Due to this nonlinear loop response, the loop gain increases excessively and saturates easily as I_{SiPM} increases. To solve this problem, we implement a PWM generator that produces V_{DT} whose duty is a square-root function of V_E, by comparing V_E with a quadratic sawtooth waveform (V_{QST}) [see Fig. 6(b)]. In this case, when V_E doubles, the duty of V_{DT} increases by $\sqrt{2}$ times, and thus, Q_{OUT} doubles, resulting in a linear loop response. In addition, the gain of the PWM generator with the proposed V_{QST} generator will be changed $1/V_M$ to a square root of $1/V_M$. The proposed quadratic sawtooth waveform generator can be implemented simply as shown in the schematic diagram in Fig. 7. First, if constant I_{ST} flow to C_{ST}, V_{ST} with linear slope can be generated. And then, since V_{ST} is used as a reference voltage of the regulated cascode circuit, I_{SQ} increases linearly at the ratio of V_{ST} and R_{QST}. Finally, by pouring I_{SQ} to C_{QST}, V_{QST} can be generated as a function of squared versus time. In other words, after converting V_{ST} to I_{ST}, V_{QST} is finally obtained by integrating with respect to the time axis. The regulated cascode current mirror circuits including the error AMP are only responsible for converting V_{ST} to I_{ST} with R_{QST}.

Fig. 8(a) shows the complete implementation result of the proposed mobile radiation dosimeter. The simple 4-b duty quantizer

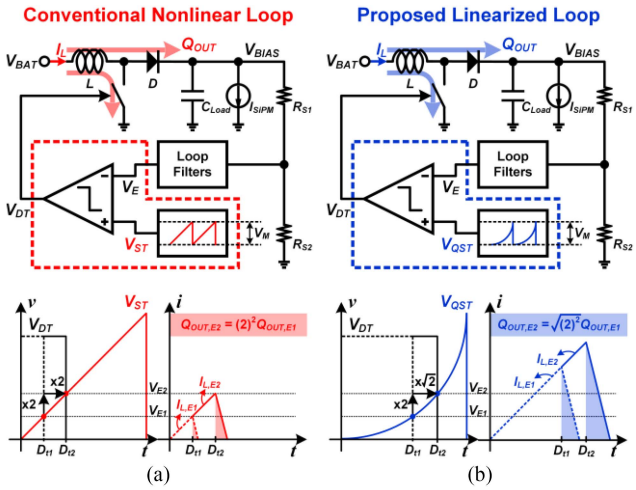

Fig. 6. (a) Conventional nonlinear PWM control loop with a sawtooth waveform generator. (b) Proposed linearized PWM control loop with a quadratic sawtooth waveform generator.

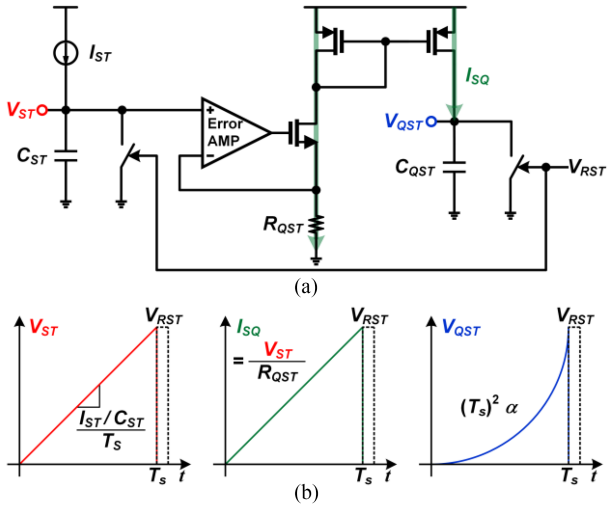

Fig. 7. Proposed quadratic sawtooth waveform generator. (a) Detailed circuit implementation. (b) Output waveforms.

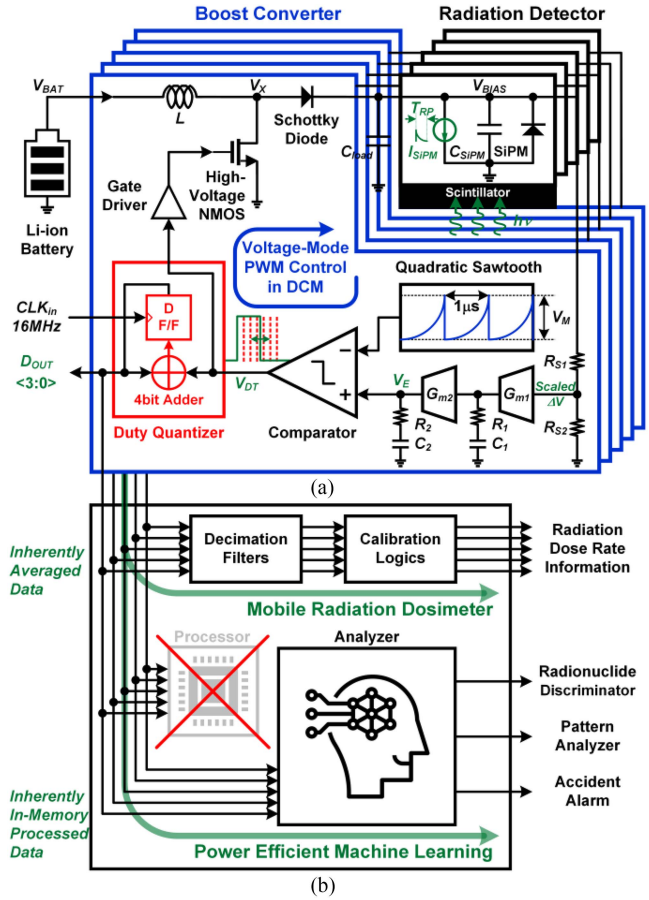

Fig. 8. Proposed mobile radiation dosimeter. (a) Complete implementation with a duty quantizer. (b) Various applications in post-processing.

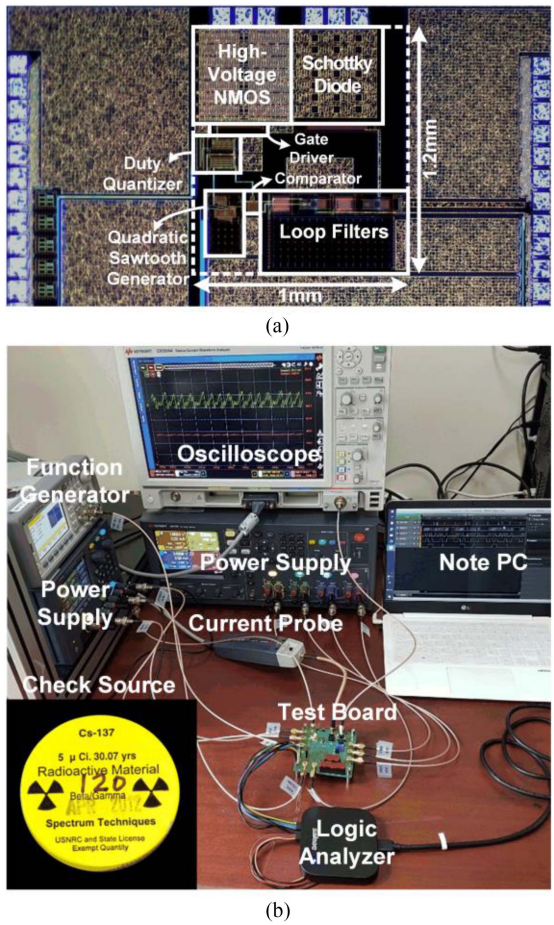

Fig. 9. (a) Die photograph. (b) Measurement setup for proposed mobile radiation dosimeter.

that quantizes V_{DT} can serve as an analog-to-digital converter of the sensor interface circuits. The PWM output is quantized to 4 b. As the switching frequency is 1 MHz, the clock for the counter in the quantizer is 16 MHz. In this implementation, the 1MHz switching clock is generated from the 16 MHz external clock signal used by the counter. Employing the PWM control, the amount of Q_{OUT} increases quadratically with the duty of V_{DT} when operating in DCM. As a result, the I_{SiPM} value can be obtained from ${D_{\mathrm{OUT}}}^2$. It means that the digitized I_{SiPM} information is provided inherently in the process of regulating V_{BIAS} to operate the SiPM.

Fig. 8(b) shows various applications of the proposed mobile radiation dosimeter. First, the 4-b D_{OUT} data in Fig. 8(a) provide radiation dose rate information through a back-end system composed of decimation filters and calibration logic. In particular, unlike conventional radiation sensor interface circuits, D_{OUT} data exhibits inherently averaged characteristics by G_m–C loop filters. Therefore, it lowers the complexity of the decimation filter system and helps to quickly output exposure dose information. Second, the structure proposed in this article is expected to be effectively applied to radiation machine learning systems such as in [21], [22], [23], and [24]. However, these system architectures had no choice but to be excessively oversized because the conventional radiation sensor interface circuits simply transmit only the amount of energy of radiation particles and the number of radiation events per period. In the process of learning the radiation signal information obtained from the conventional radiation sensor interface circuits to the back-end system, excessive power is inevitably consumed. On the other hand, Since D_{OUT} obtained from the radiation detection system proposed in this article has already been averaged during the cycle of $\mathrm{CLK_{in}}$, the process of learning the sensed data to the memory can be eliminated. In other words, the radiation signal processed through the proposed radiation detection system has a built-in preprocessing function. Therefore, it will be possible to analyze the output data and make decisions only with a simple analyzer system without a complex processor.

IV. Measurement Results

Fig. 9 shows the die photograph and setup for measuring the performance of the proposed mobile radiation dosimeter. Fabricated in a 180-nm Bipolar CMOS DMOS process, the proposed readout IC occupies only 1.2 mm^2 area [see Fig. 9(a)] while incorporating both the sensor interface and power management functions on-chip, unlike previous works. Since the

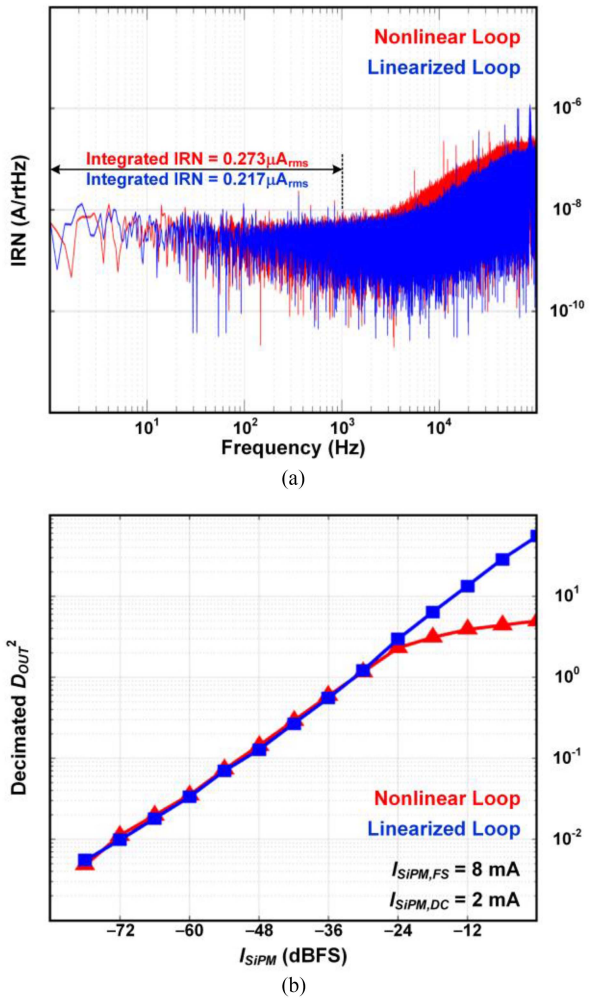

Fig. 10. Measured electrical performance. (a) Input-referred noise (IRN). (b) Linear input current range.

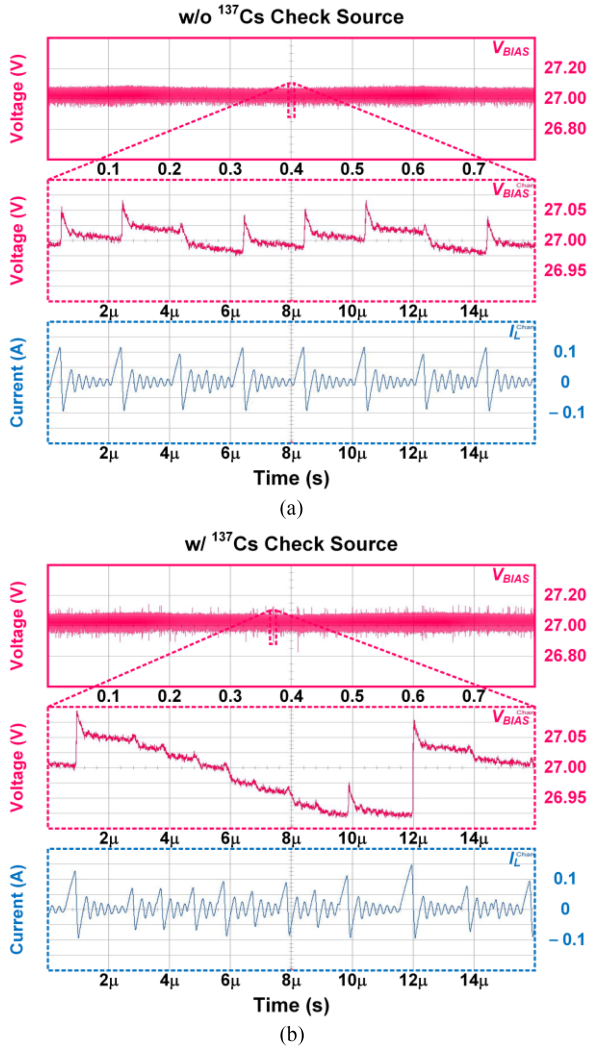

Fig. 11. Measured transient response (a) with and (b) without radiation check source (^{137}Cs).

implemented prototype IC is a hybrid structure composed of a dc–dc boost converter and an analog-to-digital converter, various measurement equipment was used to accurately measure each performance [see Fig. 9(b)]. First, D_{OUT} containing radiation signal information is transmitted to the note PC through the logic analyzer. A clock signal synchronized with D_{OUT} is delivered in parallel, making it easy for logic analyzers to postprocess. Second, V_{BAT} and voltages of subblocks are supplied from the multioutput power supply to measure the efficiency performance of the proposed boost converter. Third, the inductor current (I_L) can be measured while the proposed boost converter is operating normally, using a commercial current probe. Fourth, to accurately measure the performance of the proposed SiPM readout circuits, an irradiation test using a radiation check source (^{137}Cs) was performed. For more accurate measurements, the external visible light was completely blocked so that the SiPM did not generate an abnormally large amount of dark current.

Fig. 10 shows the electrical measurement results of the proposed SiPM readout IC. The integrated IRN is measured to be 0.273 $\mu\mathrm{A}_{\mathrm{rms}}$ and 0.217 $\mu\mathrm{A}_{\mathrm{rms}}$ over 1-kHz noise bandwidth when V_E is compared with V_{ST} and V_{QST}, respectively. It verifies that the implemented SiPM readout IC achieves sufficiently low IRN, which is lower than the dark current level of SiPM [12]. Since the results in Fig. 10(a) are measured when I_{SiPM} is small, it cannot be said that the quadratic sawtooth generator has a dramatic effect in terms of noise performance. However, in Fig. 10(b), the decimated $D_{\mathrm{OUT}}{}^2$ values plotted as a function of I_{SiPM} show a noticeable effect in the current range where I_{SiPM} is large enough. We can find that the linear sensing region can be extended significantly by linearizing the loop response.

The measured V_{BIAS} and I_L waveforms are shown in Fig. 11. The proposed readout IC embedded in a boost converter converts 3.7 V of V_{BAT} to 27 V of V_{BIAS}, operating the SiPM with sufficiently high voltage applied. Without any radioactive check source around, the boost converter drives the SiPM operating in standby mode by supplying the dark current generated by the SiPM [see Fig. 11(a)]. However, the boost converter switches slower than 1 MHz in the waveform of Fig. 11(a). This can be explained by the result that the pulse skipping mode is operated on time. Thanks to the pulse skipping mode, the boost converter always operated with high efficiency even when the amount of dark current flowing in SiPM is smaller than expected. For

TABLE I
PERFORMANCE COMPARISONS

	NSS/MIC 2017 [5]	NSS/MIC 2018 [6]	TRPMS 2017 [5]	TNS 2018 [8]	This Work [25]	MAX618 [11]	MAX5026 [13]	MAX15032 [14]	MAX15059 [15]
Process	N / A	350 nm CMOS	350 nm CMOS	350 nm CMOS	180 nm BCD	BiCMOS	BiCMOS	BiCMOS	BiCMOS
Application	SiPM Readout	SiPM Readout	SiPM Readout	SiPM Readout	Mobile Dosimeter	Industry	APD Biasing	APD Biasing	APD Biasing
Front-End Architecture	I-Conveyor + Integrator	I-Conveyor + Integrator	I-Conveyor + Integrator	CSA + Peak Detector	Duty Quantizer	N / A	N / A	N / A	N / A
Area/Ch.	N / A	1.125 mm^2	1.125 mm^2 (Est.)	0.04 mm^2	1.2 mm^2	N / A	N / A	N / A	N / A
Noise BW	N / A	N / A	N / A	N / A	1kHz	N / A	N / A	N / A	N / A
Integrated IRN	N / A	N / A	N / A	N / A	0.217 μA_{rms}	N / A	N / A	N / A	N / A
Maximum Linear Input Current Range	N / A	N / A	N / A	N / A	10mA	N / A	N / A	N / A	N / A
Power Dissipation for Readout	18mW/Ch. (Est.)	N / A	8mW/Ch.	3mW/Ch.	0mW/Ch.	N / A	N / A	N / A	N / A
Power Management Circuits	X	O (Ext. Board)	X	X	O (ASIC)	N / A	N / A	N / A	N / A
Control Mode	N / A	N / A	N / A	N / A	Voltage Mode PWM	Current Mode PWM	Current Mode PWM	Current Mode PWM	Current Mode PWM
V_{BIAS} / V_{BAT}	N / A	N / A	N / A	N / A	~27V/3.7V	~28V/3V	~36V/3V	~36V/2.7V	~76V/2.8V
CLK_{in}	N / A	N / A	N / A	N / A	1 M Hz	250 kHz	500 kHz	500 kHz	400 kHz
Load Range	N / A	N / A	N / A	N / A	1–10 mA	~500 mA	~10 mA	~20 mA	~4.5 mA
C_{Load}	N / A	N / A	N / A	N / A	16 nF	10 μF	1 μF	2.2 μF	0.1 μF
L	N / A	N / A	N / A	N / A	10 μH	40 μH	47 μH	4.7 μH	1.5 μH
Peak Efficiency	N / A	N / A	N / A	N / A	72%	75% (10 mA)	63% (5 mA)	72% (10 mA)	66% (4 mA)

example, when V_E is too low, the counter of the duty quantizer does not count as least significant bit. Therefore, the proposed duty quantizer operates in pulse skipping mode to reduce unnecessary power consumption. The boost converter operation is also measured by placing a ^{137}Cs check source closely. The plot in Fig. 11(b) shows V_{BIAS} and I_L waveforms in the case where the radiation particles are injected successively at short time intervals. Even when the check source is placed very closely, V_{BIAS} is recovered fast enough not to fall below the minimum required operating voltage of SiPM. Through this measurement result, it can be confirmed that the proposed boost converter can stably drive the SiPM in a real irradiation test, even though a relatively small C_{Load} is used.

Table I shows the performance summary and comparison table. The implemented boost converter not only generates a 27 V output voltage reliably to operate the SiPM over a load range from 1 to 10 mA but also reads I_{SiPM} out by converting V_{DT} into D_{OUT}. Thanks to the systematic concept, the additional power consumption of sensor interface circuits can be completely removed. In addition, it can be confirmed that the proposed boost converter was able to achieve sufficiently high efficiency and conversion ratio even compared to the commercial step-up converters [11], [13], [14], [15].

V. CONCLUSION

In this article, a power- and hardware-efficient radiation detection system can be proposed to prolong the battery life. By analyzing the operation principle of the radiation detection system in detail, it was possible to eliminate unnecessary power and hardware. Incorporating the duty quantizer into the boost converter, which is essential for driving the SiPM, the sensor interface circuits are no longer needed. Utilizing our proposed concept, the mobile radiation dosimeter system could achieve high efficiency in terms of power and hardware. First, it can be proven that the power consumption of the system can be prominently reduced by at least 3 mW [8] and up to 18 mW [5] because the power consumption of the sensor interface circuits can be completely saved. Second, the power optimized for SiPM performance can be supplied without using a separate off-chip power board. Lastly, cost savings of over 48% can be achieved, thanks to the saved area used for the sensor interface circuits. Because, if the sensor interface circuits occupying 1.125 mm^2 do not have to be designed, we only need to design a boost converter that takes up only 1.2 mm^2 [25]. Thanks to the inherently averaged D_{OUT}, the proposed radiation signal processing system automatically enables power-efficient signal processing.

By performing the electrical measurements, the performance of the proposed radiation detection system was sufficiently verified to replace the conventional structure. Through utilizing a commercial SiPM as a radiation detector, it was confirmed that the proposed boost converter can supply V_{BIAS} and I_{SiPM} stably. Ultimately, the proposed sensor signal processing technology is expected to be applied to all photodiode-based sensors that utilize current signals.

This research, which is the extended version of [25], has infinite potential to be developed into various research topics in the future. First, it is necessary to further increase the power conversion efficiency by utilizing various technologies of power electronics. Second, the design of the boost converter with a wide load range for a radiation detector that can detect stronger radiation could also be developed. Lastly, the novel concept can also be developed into the next challengeable research for various current-based sensors, including SiPM.

ACKNOWLEDGMENT

The chip fabrication and EDA tool were supported by the IC Design Education Center (IDEC), South Korea.

REFERENCES

[1] R. C. Baumann, "Determining the impact of alpha-particle-emitting contamination from the Fukushima Daiichi disaster on Japanese semiconductor manufacturing sites," *IEEE Trans. Nucl. Sci.*, vol. 59, no. 4, pp. 1186–1196, Aug. 2012.

[2] H. Altomonte, "Japan's nuclear disaster: Its impact on electric power generation worldwide," *IEEE Power Energy Mag.*, vol. 10, no. 3, pp. 94–96, May/Jun. 2012.

[3] Ministry of the Environment, Government of Japan, "Radiation around us: Comparison of exposure doses," Mar. 2015. [Online]. Available: https://www.env.go.jp/en/chemi/rhm/basic-info/1st/pdf/basic-1st-02-05-12.pdf

[4] Y. Ishigaki, Y. Matsumoto, R. Ichimiya, and K. Tanaka, "Development of mobile radiation monitoring system utilizing smartphone and its field tests in Fukushima," *IEEE Sens. J.*, vol. 13, no. 10, pp. 3520–3526, Oct. 2013.

[5] G. L. Montagnani, F. Sancandi, G. Cozzi, C. Fiorini, L. Buonanno, and M. Carminati, "GAMMA: An 8-channel high dynamic range ASIC for SiPM-based readout of large scintillators," in *Proc. IEEE Nucl. Sci. Symp. Med. Imag. Conf.*, 2017, pp. 1–3.

[6] L. Buonanno, M. Carminati, D. D. Vita, M. Grandi, G. L. Montagnani, and C. Fiorini, "LAILA: A compact high-dynamic range readout for high-density SiPM arrays," in *Proc. IEEE Nucl. Sci. Symp. Med. Imag. Conf.*, 2018, pp. 1–3.

[7] P. Trigilio, P. Busca, R. Quaglia, M. Occhipinti, and C. Fiorini, "A SiPM-readout ASIC for SPECT applications," *IEEE Trans. Radiat. Plasma Med. Sci.*, vol. 2, no. 5, pp. 404–410, Sep. 2018.

[8] P. Dorosz, M. Baszczyk, W. Kucewicz, and Ł. Mik, "Low power front-end ASIC for silicon photomultiplier," *IEEE Trans. Nucl. Sci.*, vol. 65, no. 4, pp. 1070–1078, Apr. 2018.

[9] X. Cheng, K. Hu, and Y. Shao, "Dual-polarity SiPM readout electronics based on 1-bit sigma-delta modulation circuit for PET detector applications," *IEEE Trans. Nucl. Sci.*, vol. 66, no. 9, pp. 2107–2113, Sep. 2019.

[10] Y. Tang, R. Zhang, and J. Chen, "A low-power 16-channel SiPM readout front-end with a shared SAR ADC in 180 nm CMOS," in *Proc. Int. Conf. Solid-State Integr. Circuit Technol.*, Nov. 2020, pp. 1–3.

[11] M. Wonders, D. L. Chichester, and M. Flaska, "Assessment of performance of new-generation silicon photomultipliers for simultaneous neutron and gamma ray detection," *IEEE Trans. Nucl. Sci.*, vol. 65, no. 9, pp. 2554–2564, Sep. 2018.

[12] On Semiconductor, "Silicon photomultipliers (SiPM), high PDE and timing resolution sensors in a TSV package," J-Series SiPM datasheet, Dec. 2018.

[13] Maxim Integrated, "28 V Internal switch, Step-up DC-DC converter," MAX618 datasheet, Apr. 2015.

[14] Maxim Integrated, "28 V, low-power, high-voltage, boost or inverting DC-DC converter," MAX629 datasheet, Oct. 2020.

[15] Maxim Integrated, "500 kHz, 36 V output, SOT23, PWM step-up DC-DC converters," MAX5028 datasheet, Mar. 2009.

[16] Maxim Integrated, "500 kHz, 36 V output, 600 mW PWM step-up DC-DC converter," MAX15032 datasheet, Aug. 2008.

[17] Maxim Integrated, "76 V, 300 mW boost converter and current monitor for APD bias applications," MAX15059 datasheet, Sep. 2020.

[18] R. W. Erickson and D. Maksimovic, *Fundamentals of Power Electronics*. Norwell, MA, USA: Kluwer, 2001.

[19] J. Roh, "High-performance error amplifier for fast transient DC-DC converters," *IEEE Trans. Circuits Syst. II, Exp. Briefs*, vol. 52, no. 9, pp. 591–595, Sep. 2005.

[20] A. K. P. Viraj and G. A. J. Amaratunga, "A monolithic CMOS 5 V/1 V switched capacitor DC-DC step-down converter," in *Proc. IEEE Power Electron. Spec. Conf.*, 2007, pp. 2510–2514.

[21] S. Jhung, S. Hur, G. Cho, and I. Kwon, "A neural network approach for identification of gamma-ray spectrum obtained from silicon photomultipliers," *Nucl. Instrum. Methods Phys. Res. A, Accel. Spectrom. Detect. Assoc. Equip.*, vol. 954, Feb. 2020, Art. no. 161704.

[22] C. Fu, A. Di Fulvio, S. D. Clarke, D. Wentzloff, S. A. Pozzi, and H. S. Kim, "Artificial neural network algorithms for pulse shape discrimination and recovery of piled-up pulses in organic scintillators," *Ann. Nucl. Energy*, vol. 120, pp. 410–421, 2018.

[23] T. S. Sanderson, C. D. Scott, M. Flaska, J. K. Polack, and S. A. Pozzi, "Machine learning for digital pulse shape discrimination," in *Proc. IEEE Nucl. Sci. Symp. Med. Imag. Conf.*, 2012, pp. 199–202.

[24] R. M. Preston, J. E. Eberhardt, and J. R. Tickner, "Neutron-gamma pulse shape discrimination using organic scintillators with silicon photomultiplier readout," *IEEE Trans. Nucl. Sci.*, vol. 61, no. 4, pp. 2410–2418, Aug. 2014.

[25] H. Jeon, I. Choi, Y. Kim, S.-U. Shin, and M. Je, "A SiPM readout IC embedded in a boost converter for mobile dosimeters," in *Proc. IEEE Symp. VLSI Circuits*, Jun. 2021, pp. 1–2.

Hyuntak Jeon received the B.S. degree in electronic and electrical engineering from Hongik University, Seoul, South Korea, in 2015, and the M.S. and Ph.D. degrees in electrical engineering from Korea Advanced Institute of Science and Technology, Daejeon, South Korea, in 2017 and 2021, respectively.

From 2021 to 2022, he was a Senior Researcher with the Agency for Defense Development, Daejeon, South Korea. In 2022, he joined the School of Electronics Engineering, Chungbuk National University, Cheongju, South Korea, where he is currently an Assistant Professor. His research interests include mixed-signal circuit designs for sensor interface IC and electrical system designs for guided ballistic missile systems.

Se-Un Shin (Member, IEEE) received the B.S. degree in electronics engineering from Kyungpook National University, Daegu, South Korea, in 2013, and the integrated M.S. and Ph.D. degrees in electrical engineering from the Korea Advanced Institute of Science and Technology, Daejeon, South Korea, in 2018.

From 2018 to 2019, he was with the University of Michigan, Ann Arbor, MI, USA, where he was involved in the development of low-power analog circuit design and automation as a Postdoctoral Associate. From 2019 to 2020, he was a Faculty with the School of Electronics and Electrical Engineering, Dankook University, Cheonan, South Korea. Since 2021, he has been with the Department of Electrical Engineering, Ulsan National Institute of Science and Technology, Ulsan, South Korea, where he is currently an Assistant Professor. His current research interests include analog-integrated circuit designs and power management IC designs, energy harvesting, battery chargers, wireless power transfer systems, switched capacitor/inductive converters, and hybrid converter topologies.